Liquid Crystals
Publication details, including instructions for authors and subscription information:
http://www.informaworld.com/smpp/title~content=t713926090

Phase transitions and rheology of aramid solutions

S. J. Picken[a]
[a] Corporate Research Department Arnhem, Akzo Research, Arnhem, The Netherlands

To cite this Article Picken, S. J.(1989) 'Phase transitions and rheology of aramid solutions', Liquid Crystals, 5: 5, 1635 — 1643
To link to this Article: DOI: 10.1080/02678298908027798
URL: http://dx.doi.org/10.1080/02678298908027798

LIQUID CRYSTALS, 1989, VOL. 5, NO. 5, 1635–1643

Phase transitions and rheology of aramid solutions

by S. J. PICKEN
Akzo Research, Corporate Research Department Arnhem, P.O. Box 9300, 6800 SB Arnhem, The Netherlands

(*Received 7 October 1988; accepted 20 January 1988*)

Clearing temperatures of solutions of poly(4-4′-benzanilidylene-terephthalamide) in concentrated sulphuric acid are presented as a function of polymer concentration and average molecular weight. The orientational order parameter $\langle P_2 \rangle$ is obtained from birefringence measurements. The experimental results are explained by a mean-field type theory similar to the Maier–Saupe model for thermotropic liquid crystals. Molecular flexibility, concentration and molecular weight are taken into account by using simple scaling factors. The birefringence induced by shear flow in an isotropic solution of poly(*para*-phenylene-terephthalamide) shows a strong pretransitional behaviour. This indicates the occurrence of a flow-induced phase transition.

1. Introduction

In lyotropic solutions of fully aromatic polyamides (or aramids) in concentrated H_2SO_4 a temperature-induced phase transition from the nematic to the isotropic phase is observed. The value of this clearing temperature depends on the polymer concentration. Understanding this combination of thermotropic and lyotropic behaviour requires the study of the molecular properties that determine the formation of the nematic phase. The occurrence of a lyotropic nematic phase in main-chain polymers is determined by molecular anisotropy, the strength of the anisotropic potential, molecular flexibility and the concentration [1–4].

Here a study of poly(4-4′-benzanilidylene-terephthalamide) (DABT, see figure 1) in concentrated H_2SO_4 is presented. The influence of the molecular weight on the concentration dependence of the clearing temperature is given. The orientational order parameter, obtained from birefringence measurements, is found to be similar to that of low molecular weight thermotropic materials. The results are explained by a simple model based on the Maier–Saupe mean-field theory. Some preliminary results are given for the birefringence induced by shear flow in an isotropic solution of poly(*para*-phenylene-terephthalamide) (PPTA, see figure 1).

2. Experimental

To determine the clearing temperature, the solutions of DABT in concentrated H_2SO_4 were investigated by polarization microscopy. We used a Leitz Orthoplan-pol. polarizing microscope with a Mettler FP80/82 hot stage. The heating rate was 5°C min^{-1}. For each solution 10 measurements of T_{ni} (the clearing temperature) were made. Here T_{ni} is the temperature at which 50 per cent phase separation is observed. The biphasic region is about 5°C wide. The average clearing temperatures are shown in figure 2 as a function of the concentration (in % (w/w)). Three different molecular

0267-8292/89 $3.00

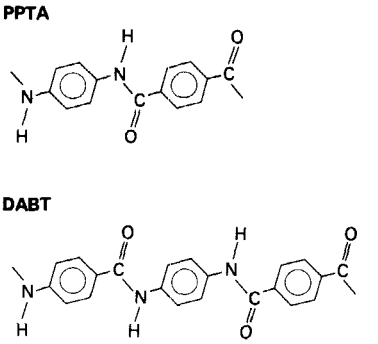

Figure 1. The studied aramids PPTA and DABT.

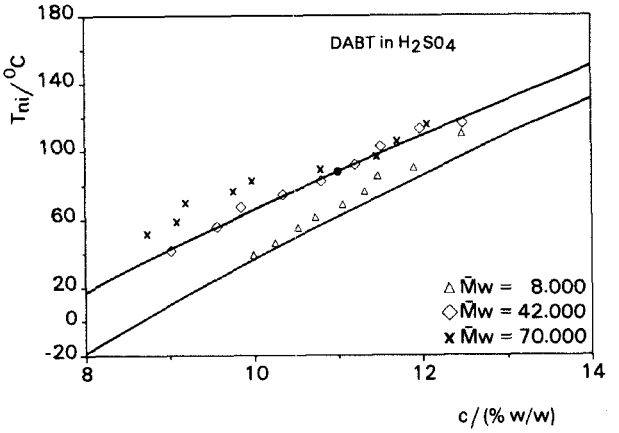

Figure 2. Clearing temperatures (T_{ni}) of DABT solutions as a function of polymer concentration and average molecular weight $\bar{M}_w$.

weights were used. The values for $\bar{M}_w$, estimated from viscosity measurements at a standardized concentration, are shown in table 1.

The results for the influence of concentration on the clearing temperature were fitted to a simple power law (T_{ni} and A in K, and c and α are scalars):

$$T_{ni} = Ac^{\alpha}. \tag{1}$$

This power law equation was chosen because for the limit $c \to 0$ we expect $T_{ni} \to 0$. In addition, de Gennes has shown that the use of scaling relations can be most instructive [5]. The results of the least squares fits are also shown in table 1. The curves in figure 2 are not the least squares fits, but are from the model described later.

Table 1. The molecular weights of the DABT samples with the parameters of the least squares fits to equation (1). The value of the standard deviation is given in parentheses.

$\bar{M}_w$	A/K	α
8000	37 (2)	0·92 (0·03)
42 000	74 (5)	0·66 (0·03)
70 000	115 (10)	0·49 (0·04)

The results show that the clearing temperature is more sensitive to concentration with low molecular weight samples. We attribute this to molecular flexibility. A low molecular weight sample will behave as a rigid rod system. A high molecular weight sample will show 'worm-like' behaviour, leading to a smaller influence of concentration.

In addition to the clearing temperature measurements, we have also performed birefringence measurements. We used solutions with a clearing temperature of about 85°C. The birefringence was determined by using an Abbe refractometer (Zeiss model B) and a thermostated oil bath. This method is described in [6]. With this technique $n_\perp$ can be determined in the nematic phase and n_{iso} in the isotropic phase. By extrapolation of the isotropic index of refraction into the nematic phase it is possible to estimate the anisotropy of the dielectric constant using

$$\Delta\varepsilon = 3(\varepsilon_{iso} - \varepsilon_\perp) = 3(n_{iso}^2 - n_\perp^2). \tag{2}$$

Here each component of the dielectric constant is just the square of the corresponding index of refraction. The value for $\Delta\varepsilon$ is expected to be proportional to the orientational order parameter $\langle P_2 \rangle$. This is discussed in more detail in [6, 7]. The values for $\langle P_2 \rangle$ as well as the anisotropy of the dielectric constant are shown in figures 3–5 as a function of $T - T_{ni}$. The curves are from theory. The broken line corresponds to the standard Maier–Saupe mean-field theory and the drawn curves from the model described in §3.

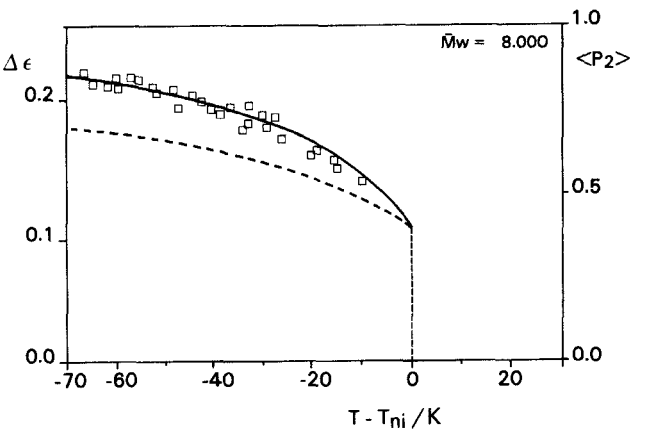

Figure 3. Anisotropy of the dielectric constant and $\langle P_2 \rangle$ as a function of the relative temperature ($T - T_{ni}$) for $\bar{M}_w = 8000$. The full curve is from the present theory. The broken curve is from the traditional Maier–Saupe model.

In principle the extrapolation of n_{iso} should also involve a correction for the density change at the nematic–isotropic transition. From measurements of $n_\parallel$ it is found that this correction can be ignored. This means that the density change at T_{ni} is small. Although an Abbe refractometer provides a simple method to determine the index of refraction, the following remarks are in order. First, some experience is required to observe the $n_\perp$ component with a refractometer. The contrast of the observed image can be improved by using an analyser to remove the extraordinary component of the transmitted light. It was found that the measurement of $n_\perp$ in aramid solutions was more difficult than with low molecular weight nematics (such as 5CB, 4-*n*-pentyl-4′-cyanobiphenyl) due to a rather low contrast. Secondly, with

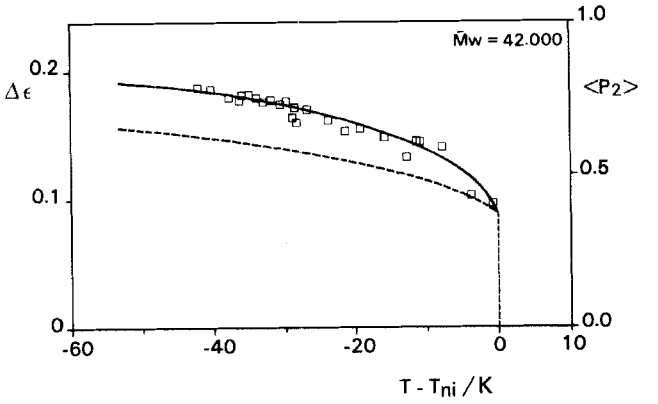

Figure 4. As figure 3, for $\bar{M}_w = 42\,000$.

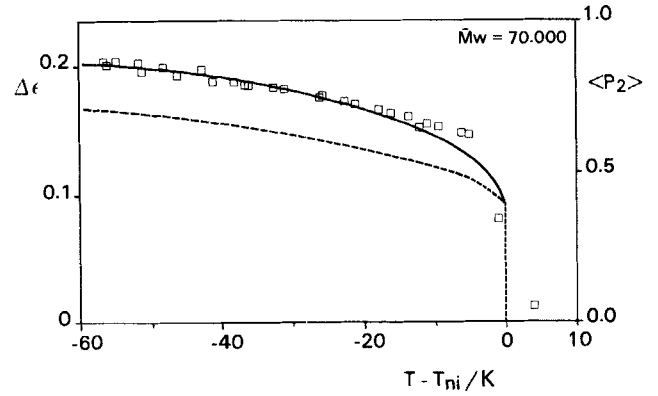

Figure 5. As figure 3, for $\bar{M}_w = 70\,000$.

aramid solutions the reproducibility of the results can be problematic. It was found that the cleaning procedure of the refractometer prisms could influence the results. This may be caused by a thin film of water adhering to the prism surface. The method we used consisted of cleaning the prisms at 60°C with acetone and subsequently inserting the aramid solution at this elevated temperature. This procedure leads to reproducible results for the refractive indices.

Finally, we have also performed some preliminary measurements of the flow-induced birefringence in an isotropic solution of PPTA. The experimental apparatus consisted of a shear-flow cell mounted on a Leitz Orthoplan-pol. polarization microscope. Details are given in [8]. The retardation (Γ) between the ordinary and the extraordinary components of the transmitted light is determined using the Sénarmont method. From the retardation, Γ, and the thickness of the sample, d, the birefringence Δn can be determined:

$$\Delta n = \Gamma/d. \tag{3}$$

The results for the measured birefringence are shown in figure 6. The thickness of the cell was 25 μm. The shear rates used are as indicated in the figure. The wavelength of the light was 547 nm. The clearing temperature of the solution was about 45°C.

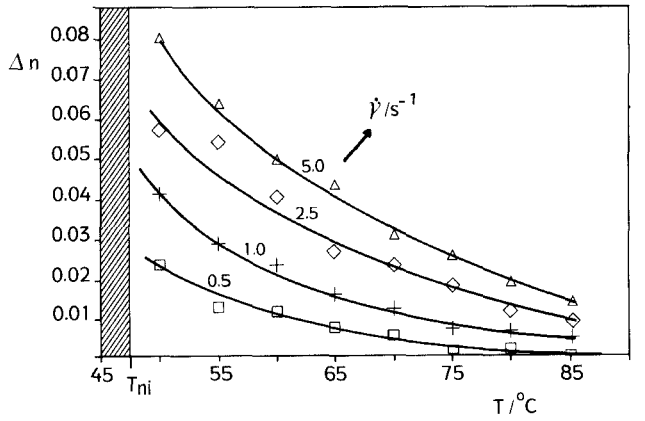

Figure 6. Birefringence induced by shear flow as a function of temperature and shear rate for an isotropic PPTA solution.

From the curves we observe that there is a strong pretransitional behaviour in the birefringence, i.e. the flow-induced birefringence in the isotropic phase increases strongly when the nematic phase is approached. The measured values for the birefringence are similar to those found in the nematic phase of the DABT solutions. This can be estimated from the approximate relation

$$\begin{aligned} \Delta\varepsilon &= \varepsilon_{\parallel} - \varepsilon_{\perp} = (\bar{n} + 2\Delta n/3)^2 - (\bar{n} - \Delta n/3)^2 \\ &= 2\bar{n}\Delta n + \Delta n^2/3 \approx 2\bar{n}\Delta n \end{aligned} \tag{4}$$

for Δn small, where $\bar{n}$ is the average index of refraction

$$\bar{n} = (n_{\parallel} + 2n_{\perp})/3. \tag{5}$$

The results indicate that applying a relatively small shear rate leads to a degree of orientational order, in the initially isotropic solution, that is comparable with the order found in the nematic phase.

3. Theory

In this section a brief description is given of a simple mean-field type model to describe the observed behaviour. The model is similar to the Maier–Saupe theory for low molecular weight thermotropic liquid crystals [9]. The present model is discussed in more detail in [4]. The standard Maier–Saupe model for nematic liquid crystals is based on the mean-field potential

$$U = -\varepsilon\langle P_2\rangle P_2(\cos\beta), \tag{6}$$

which describes the average influence of the nematic environment on the orientation of one particle. The strength of the potential is given by the parameter ε. The orientational order of the nematic environment is described by the order parameter $\langle P_2\rangle$. This is the average value of the second order Legendre polynomial of $\cos\beta$: $P_2(\cos\beta)$. In the isotropic phase $\langle P_2\rangle = 0$, whereas for perfect molecular alignment $\langle P_2\rangle = 1$.

Solving the self-consistency equation

$$\langle P_2 \rangle = \frac{\int_{-1}^{1} d(\cos\beta)\, P_2(\cos\beta) \exp(-U/(k_B T))}{\int_{-1}^{1} d(\cos\beta) \exp(-U/(k_B T))} \tag{7}$$

with the requirement that the free energy is minimal, leads to a first order phase transition from the nematic to the isotropic phase at $k_B T_{ni}/\varepsilon \approx 0{\cdot}22$.

Our extension of the Maier–Saupe model to lyotropic polymer solutions is performed by taking the influence of concentration and molecular flexibility into account by the scaling relation

$$\varepsilon = \varepsilon^* c^\gamma L^\delta(T) = \varepsilon^* c^2 L^2(T), \tag{8}$$

where c is the polymer concentration, ε^* is a scaling factor to be determined from experiments and $L(T)$ is the 'contour projection length'. Our choice for the exponents γ and δ (both 2) is based on the fact that the attractive part of the Lennard–Jones potential is proportional to $1/r^6$, which is proportional to $1/V^2$ or c^2, and that as the Maier–Saupe potential is a generalized two particle interaction we expect an L^2 dependence. In addition, we find that these values for the exponents give the best agreement with the experimental results.

The 'contour projection length' is a measure for the axial ratio of the particles. For low molecular weight materials where the molecules are essentially inflexible $L(T)$ is just the end-to-end distance of a molecule L_c (the contour length). For a high molecular weight material $L(T)$ corresponds to the persistence length L_p of the polymer. Using a worm-like model, the following form for the 'contour projection length' is obtained [4]:

$$L(T) = L_p \frac{1 - \exp(-(L_c T)/(L_p T_p))}{T/T_p}, \tag{9}$$

where T_p is the temperature at which the persistence length is measured. For a derivation of equation (9), see the appendix. Usually T_p will be approximately 20°C (293 K). A value of 29 nm is found for the persistence length of PPTA, using dynamic light scattering methods [10].

We observe that equation (9) corresponds to the persistence length L_p for high molecular weights (L_c large), with a $1/T$ temperature dependence. For low molecular weights $L(T) = L_c$, and is independent of temperature, as expected.

To solve equations (6)–(9) we used the following method. First we determined $L(T)$ from equation (9) at T_{ni} of a certain aramid solution (of known concentration, L_c is calculated using $1{\cdot}94\bar{M}_w/357$ nm). Secondly, we used the concentration and the known value of T_{ni} to calculate ε^* from equation (8), using $k_B T_{ni}/\varepsilon = 0{\cdot}22$ from the Maier–Saupe model. Thirdly, for other concentrations, temperatures and molecular weights we solved equation (7) (substituting equations (8) and (9) into equation (6) to obtain U).

4. Discussion

In our model the conformation of the polymer chain and the mean-field potential are effectively decoupled. Also, the influence of excluded volume is not taken into account. This is a rather questionable approximation for polymers with a persistence

length of about 30 nm. Despite these objections we feel that our model is justified by its simplicity and the good agreement with experiment. This can be seen from figures 2–5. The theoretical curves were obtained using a value for L_p of 35 nm (at $T_p = 293$ K), in reasonable agreement with the experimental value for PPTA. Both the influence of concentration and the molecular weight on T_{ni} are described quite well. The closed circle in figure 2 was used to determine the absolute strength of the mean-field potential, ε^* in equation (8). The T_{ni} versus concentration results for the highest molecular weight polymer sample ($\bar{M}_w = 70\,000$) are predicted to be the same as for the intermediate value ($\bar{M}_w = 42\,000$). In both cases the contour length is substantially larger than the persistence length. The measured values at high concentration support this prediction. However, at lower concentrations the agreement is not so good. This might be due to the rather slow response of high molecular weight solutions to a temperature sweep.

In figures 3–5 we observe that the temperature dependence of $\langle P_2 \rangle$ is also described well by the model. The full curves correspond to the model described here and the broken curves to the standard Maier–Saupe model. The measurements do not allow a choice to be made between the standard Maier–Saupe model and our extended model which predicts a steeper temperature dependence of $\langle P_2 \rangle$ near T_{ni}. This is partially due to the arbitrary scaling factor between $\langle P_2 \rangle$ and $\Delta\varepsilon$. The value of this scaling factor $\Delta\varepsilon_0$ is shown in table 2, where the values for $\langle P_2 \rangle$ were obtained from our model. Thus, $\Delta\varepsilon_0$ is obtained using $\Delta\varepsilon = \Delta\varepsilon_0 \langle P_2 \rangle$. The values for $\Delta\varepsilon_0/c$ shown in table 2 are found to be mutually consistent.

Table 2. The constant of proportionality $\Delta\varepsilon_0$ between $\langle P_2 \rangle$ and $\Delta\varepsilon$ for the various molecular weights of DABT.

$\bar{M}_w$	$\Delta\varepsilon_0$	c/%(w/w)	$\Delta\varepsilon_0 c^{-1}$
8000	0·26	11·4	2·3
42 000	0·24	10·8	2·2
70 000	0·25	10·3	2·4

The results for the shear-induced birefringence indicate that there is a strong coupling between the orientational distribution function and the external flow-field. The strong pretransitional behaviour can be used to estimate the contribution of shear flow on the effective (mean field) molecular potential. This could then be extended into the nematic phase to study the influence of shear rate on the orientational order. Due to the erratic 'domain flow' in the nematic phase this cannot be measured directly [11]. The very high value of the shear-induced birefringence in an isotropic PPTA solution, comparable with the values for the nematic phase, indicates the occurrence of a shear-induced phase transition.

Appendix

Derivation of the contour projection length

The polymer is modelled as a segmented chain where the rigid subsegments (of length a) are oriented parallel to each other by an orienting potential U

$$U = -\alpha \cos \Theta.$$

The orientational distribution function of a segment, assuming a fixed orientation of the previous one, is

$$f(\Theta) = \zeta^{-1} \exp\left(\frac{\alpha}{k_B T} \cos\Theta\right),$$

with

$$\zeta = \int_{-1}^{1} d(\cos\Theta) \exp\left(\frac{\alpha}{k_B T} \cos\Theta\right) = \frac{2k_B T}{\alpha} \sinh\left(\frac{\alpha}{k_B T}\right).$$

Now the average deviation angle is

$$\langle \cos\Theta \rangle = \frac{\langle \mathbf{a}_n \cdot \mathbf{a}_{n+1} \rangle}{a^2} = \zeta^{-1} \int_{-1}^{1} d(\cos\Theta) \exp\left(\frac{\alpha}{k_B T} \cos\Theta\right) \cos\Theta.$$

Assuming that the correlation between subsequent subsegments is large, i.e. $\alpha/k_B T$ is large, we find

$$\langle \cos\Theta \rangle = \coth\left(\frac{\alpha}{k_B T}\right) - \frac{k_B T}{\alpha} \approx 1 - \frac{k_B T}{\alpha}.$$

The condition mentioned above can be satisfied by choosing a sufficiently small length of a subsegment. The persistence length is obtained from

$$L_p(T) = a \sum_{n=0}^{\infty} \langle \cos\Theta \rangle^n = \frac{a}{1 - \langle \cos\Theta \rangle} = \frac{\alpha a}{k_B T}.$$

Thus, it follows that

$$L_p(T) \propto 1/T,$$

i.e. the persistence length is proportional to the reciprocal of the temperature.

For a finite chain we derive similarly ($L_c = Na$)

$$L(T) = a \sum_{n=0}^{N-1} \langle \cos\Theta \rangle^n = \frac{L_c}{N} \frac{1 - [\coth(\alpha/(k_B T)) - k_B T/\alpha]^N}{1 - [\coth(\alpha/(k_B T)) - k_B T/\alpha]}.$$

Now, taking the continuous limit where $N \to \infty$, $\alpha \to \infty$ and $\alpha = KN$,

$$L(T) = \lim_{\substack{N \to \infty \\ \alpha = KN}} \frac{L_c}{N} \frac{1 - (1 - k_B T/(NK))^N}{1 - (1 - k_B T/(NK))} = L_c \frac{1 - \exp(-k_B T/K)}{k_B T/K}.$$

Requiring that $L(T_p) = L_p$ (the persistence length at temperature T_p) for an infinite chain length, we find that

$$K = (L_p/L_c) k_B T_p$$

and thus

$$L(T) = L_p \frac{1 - \exp(-(L_c T)/(L_p T_p))}{T/T_p}.$$

References

[1] KHOCHKLOV, A. R., and SEMENOV, A. N., 1985, *J. statist. Phys.*, **38**, 161.

[2] TEN BOSCH, A., MAISSA, P., and SIXOU, P., 1983, *Phys. Lett.* A, **94**, 298. *J. chem. Phys.*, **79**, 3462 (1983). *J. Phys., Paris, Lett.*, **44**, L105 (1983).

[3] WARNER, M., GUNN, J. M. F., and BAUMGARTNER, A., 1985, *J. Phys.* A, **18**, 3007.
[4] PICKEN, S. J., *Macromolecules* (submitted).
[5] DE GENNES, P. G., 1979, *Scaling Concepts in Polymer Physics* (Cornell University Press).
[6] DE JEU, W. H., 1980, *Physical Properties of Liquid Crystalline Materials* (Gordon & Breach).
[7] VERTOGEN, G., and DE JEU, W. H., 1988, *Thermotropic Liquid Crystals, Fundamentals* (Springer-Verlag).
[8] BLOK, P., PICKEN, S. J., and VERWAAIEN, H. H. T., 1987, *Constructeur*, **26**(12), 44 (in Dutch).
[9] MAIER, W., and SAUPE, A., 1960, *Z. Naturf.*, **149**, 882. *ibid.* **159**, 187.
[10] YING, Q., and CHU, B., 1984, *Makromolek. Chem. rap. Commun.*, **5**, 785.
[11] DOPPERT, H. L., and PICKEN, S. J., 1987, *Molec. Crystals liq. Crystals*, **153**, 109.